Journal of Biomedical Optics

SPIEDigitalLibrary.org/jbo

Applicability of confocal laser scanning microscopy for evaluation and monitoring of cutaneous wound healing

Susanne Lange-Asschenfeldt
Adrienne Bob
Dorothea Terhorst
Martina Ulrich
Joachim Fluhr
Gil Mendez
Hans-Joachim Roewert-Huber
Eggert Stockfleth
Bernhard Lange-Asschenfeldt

SPIE

Applicability of confocal laser scanning microscopy for evaluation and monitoring of cutaneous wound healing

Susanne Lange-Asschenfeldt, Adrienne Bob, Dorothea Terhorst, Martina Ulrich, Joachim Fluhr, Gil Mendez, Hans-Joachim Roewert-Huber, Eggert Stockfleth, and Bernhard Lange-Asschenfeldt
Charité University Medicine Berlin, Department of Dermatology, Skin Cancer Center Charité, Universitätsmedizin Berlin, Charité Campus Mitte, Charitéplatz 1, 10117 Berlin, Germany

Abstract. There is a high demand for noninvasive imaging techniques for wound assessment. *In vivo* reflectance confocal laser scanning microscopy (CLSM) represents an innovative optical technique for noninvasive evaluation of normal and diseased skin *in vivo* at near cellular resolution. This study was designed to test the feasibility of CLSM for noninvasive analysis of cutaneous wound healing in 15 patients (7 male/8 female), including acute and chronic, superficial and deep dermal skin wounds. A commercially available CLSM system was used for the assessment of wound bed and wound margins in order to obtain descriptive cellular and morphological parameters of cutaneous wound repair noninvasively and over time. CLSM was able to visualize features of cutaneous wound repair in epidermal and superficial dermal wounds, including aspects of inflammation, neovascularisation, and tissue remodelling *in vivo*. Limitations include the lack of mechanic fixation of the optical system on moist surfaces restricting the analysis of *chronic skin wounds* to the wound margins, as well as a limited optical resolution in areas of significant slough formation. By describing CLSM features of cutaneous inflammation, vascularisation, and epithelialisation, the findings of this study support the role of CLSM in modern wound research and management. [DOI: 10.1117/1.JBO.17.7.076016]

Keywords: *in vivo* reflectance confocal microscopy; noninvasive skin imaging; wound healing.

Paper 11653 received Nov. 6, 2011; revised manuscript received Jun. 3, 2012; accepted for publication Jun. 7, 2012; published online Jul. 9, 2012.

1 Introduction

Skin wounds comprise a broad spectrum of clinical manifestations, depending on their aetiology, clinical course, and anatomic location as well as individual pathophysiologic factors. Routine wound bed assessment is based on the clinical evaluation of wound characteristics such as size, location, the presence of cavities, sinuses, and fistulae. Other features may include the presence of necrosis, granulation, infection, or other signs of critical colonization.[1] Besides assessment of the wound area itself, the condition of surrounding skin is of crucial importance. Wound margins may present oedematous, white, shiny, warm, red, dry, or scaling ultimately serving as prognostic factors for the individual healing capacity.[2] While visual inspection is the established procedure in clinical dermatology, the method is inherently subjective, often yielding inaccurate descriptions of wound conditions, and do not permit an ultrastructural analysis of the wound tissue.[3]

In that regard, routine histology remains the gold standard for morphologic evaluation of cutaneous wound healing.[4] However, while histology still plays an important role in skin research and the development of innovative wound dressings, there are substantial limitations. The invasive character of biopsies does not allow an assessment over time and the method may not be feasible for evaluation of large or recurrent wounds or patients with significant impairment of wound healing or high risk of infection. Lastly, tissue removal and histological processing may result in artifacts, further limiting its clinical applicability.

On the other hand, wound healing has been extensively studied in a variety of animal species including amphibians, rodents, and pigs. Animal models allow the infliction of skin wounds under standardized conditions and an investigation of the influence of pharmacological and physical treatments on tissue repair.[5] For investigational purposes rodents can be genetically modified to over-express cytokines of interest thereby gaining new insights on their respective influence on cutaneous wound healing.[6–8] There are, however, significant differences in tissue repair between the species, such that regenerative capacities of amphibians cannot be compared to wound healing in mammals and rodents. Therefore, the model has to be carefully chosen and experiments in human skin still represent the gold standard for research in the field of tissue repair.

Considering these limitations, a number of noninvasive imaging techniques have been evaluated for their applicability for assessment of human skin wounds at different stages of wound healing.[9] Among them, *in vivo* reflectance confocal laser scanning microscopy (CLSM) represents an innovative optical imaging tool for noninvasive evaluation of normal and diseased skin *in vivo* and in real time. Previous reports have shown its diagnostic suitability for inflammatory, neoplastic, and proliferative skin disorders[7] and its applicability to study skin diseases over time.[10] Altintas and co-workers have first employed CLSM for evaluation of burn wounds in human volunteers, whereby aspects of microcirculation, inflammation, and histomorphology have been described.[11,12] Their findings supported the use of CLSM as an adjunctive tool for evaluation and management of burn wounds.

Address all correspondence to: Bernhard Lange-Asschenfeldt, Charité University Medicine Berlin, Department of Dermatology, Charitéplatz 1, 10117 Berlin, Germany. Tel: +49-30 450 618728; Fax: +49-30 450 518 933; E-mail: bernhard.lange-asschenfeldt@charite.de.

0091-3286/2012/$25.00 © 2012 SPIE

Based on these findings, the present study was designed to test the feasibility of *in vivo* reflectance CLSM for evaluation of skin wounds, including acute and chronic, superficial and deep dermal skin wounds in this noninvasive analysis. We used CLSM for assessment of wound bed and wound margins in order to obtain descriptive cellular and morphological parameters of cutaneous wound repair noninvasively and over time. By means of analyzing features of cutaneous inflammation, vascularisation, and epithelialisation as biomorphological endpoints of therapy, the goal of this evaluation was to study the role of CLSM in modern wound management.

2 Materials and Methods

2.1 *Patients and Study Procedures*

2.1.1 *Study participants*

The research protocol was approved by the Charité University Hospital Subcommittee on Human Studies, at the Institutional Review Board. A total of 15 patients (8 male, 7 female, SPT I-III, aged 29 to 82) were enrolled in this clinical evaluation and assigned to the individual study goals (Table 1). Written consent was obtained prior to enrollment and all clinical investigation was conducted according to GCP and the Declaration of Helsinki principles. All 15 subjects completed the study, and data of all subjects were included in the analysis.

2.1.2 *Study groups*

Group I (superficial epidermal wounds): To study the events of cutaneous wound repair following cryosurgery a total of ($n = 5$) healthy volunteers were included; each participant was treated with contact cryosurgery at −32 °C for 10 s on the volar forearm, followed by removal of the blister roof on day 1 after cryosurgery. Clinical and CLSM evaluation were performed at baseline (day 0) and follow-up (at days 1, 2, 7, 14, and week 4 ± 2 days, respectively).

Group II (superficial dermal wounds): To evaluate the healing of deeper wounds involving epidermis and dermis, the respective donor sites of skin grafts from ($n = 5$) patients undergoing skin transplantation were included. Patients were recruited from the skin surgery unit at the Department of Dermatology, Venereology, and Allergology at the Charité University Hospital (Berlin, Germany) and seen for their routine surgical care and follow-up. Clinical and CLSM evaluation were performed at baseline and follow-up at skin graft donor sites at day 5. Superficial dermal skin wounds were created by a split skin grafting procedure, using an electric dermatome (GA 630, Aesculap, Tuttlingen, Germany), whereby skin grafts of uniform thickness of approximately 0.3 mm were obtained for surgical reconstruction following the removal of skin cancer. This procedure was performed under local anesthesia.[13]

This model was chosen since the surgical use of the dermatome creates wounds at standardized depths involving the dermis stimulating the proliferation and migration of fibroblasts, myofibroblasts, and endothelial cells within the wound bed. Evaluations were not performed until day 5, since the wound bed is covered by a sterile dressing until that time point.

Group III (deep dermal wounds): To study the events of cutaneous wound repair in chronic skin ulcers a total of ($n = 5$) patients were included for evaluation. Patients were recruited from the outpatient wound clinic at the Department of Dermatology, Venerology, and Allergology at the Charité University Hospital (Berlin, Germany) where they were seen for treatment of chronic leg ulcers due to chronic venous insufficiency (Widmer stage III). All patients were treated according to the guidelines of modern wound managements.[14] The individual response to the conservative wound bed preparation was graded: poor (no response within 4 weeks), moderate (some visible signs of epithelialization at the wound margin), and good (epithelialization and decreasing wound size). Clinical and noninvasive evaluation by CLSM was performed at baseline and consecutive follow-ups up to 4 weeks following inclusion.

2.2 *Confocal Laser Scanning Microscopy*

CLSM evaluation was performed using a commercially available system (Vivascope 1500®, Mavig GmbH, Munich, Lucid-Tech Inc., Henrietta, NY).[15] A detailed description of the technique and the device used has been published previously.[16,17] Briefly, the system employs an 830 nm Diode laser, generating a power of less than 30 mW at tissue level. CLSM imaging is based on tissue illumination and detection of scattered and reflected light through a small aperture, thereby producing the high lateral resolution of CLSM images, which lies around 0.5 to 1 microns. Axial resolution (optical section thickness) is about 3 to 5 microns. Optical sectioning is performed from superficial to deeper layers, by progressively moving the focus of the objective down the z-axis. Images

Table 1 Study groups and procedures. Procedures and evaluations timepoints in study group 1 (epidermal wounds), study group 2 (superficial dermal wounds), and study group 3 (deep ulcers).

Study groups	Study participants	Study procedures	Evaluation site	Evaluation time point
Group I	Healthy individuals (4F/1 M)	Contact cryosurgery at −32 °C for 10 seconds on the volar forearm, Removal of blister roof Clinical exam, serial CLSM evaluation	Wound area and surrounding skin	Days 0, 1, 2, 7, 14, 28
Group II	Patients with skin cancer receiving split skin grafts(4F/1 M)	Routine tumor excision followed by split skin graftsClinical exam, serial CLSM evaluation of the skin graft donor site	Wound area, wound margin	Day 5
Group III	Patients with chronic leg ulcers(2F/3 M)	Routine wound management with serial follow-up; clinical exam, CLSM evaluation of wound margins	Wound margin	Serial evaluations during therapeutic follow-up

are resolved in grey-scale and imaging is performed at video-rate (real-time) at 9 frames per second.

The size of individual images obtained in the horizontal plane (x-y direction) is 500×500 microns; the microscope permits horizontal mapping (Vivablockfi function) of areas from 1×1 mm to 8×8 mm and vertical mapping (Vivastack® function) whereby the system allows software-assisted imaging using pre-set or individually programmed imaging steps and penetration depths. Imaging depth (z-axis) was determined for study group 1 (superficial epidermal wounds) relative to the surface by zeroing the micrometer at the most superficial discernable skin layer. In study groups II and III imaging depth was restricted due to exudation and crust formation. In these study groups respective depths were assessed by the morphological appearance of the investigated tissue.

2.3 *CLSM Evaluation Parameters*

In each participant, one or more skin sites were selected for imaging following clinical examination; for each skin site, a systematic horizontal mapping was performed and four to six individual images were captured in axial sections beginning with the stratum corneum (SC), through the entire epidermis, and into the upper reticular dermis.

CLSM evaluation parameters included features of cutaneous wound repair on a cellular, morphological and architectural level, as well as the documentation of dynamic processes such as blood flow and inflammation, and the successive events of wound healing. CLSM evaluation parameters for respective study groups are listed in Table 2.

2.4 *Image Analysis*

All images underwent descriptive morphological analysis, including a second, retrospective analysis by an expert in the field. CLSM features of inflammation, vascularization and re-epithelialization were based on those previously published for CLSM,[18] and/or in correlation with established histological features,[19] and described in comparison to normal skin. Image analysis was performed by using a simple present/absent scheme. Semiquantitative image analysis was performed for the presence of inflammatory cells for chronic skin wounds; respective grading ranged from 0 = none, 1 = mild, 2 = moderate, and 3 = severe based on the number of detected inflammatory cells/per field of view. At least 4 to 6 images were analyzed per wound.[18]

3 Results

3.1 *CLSM Findings of Superficial Epidermal Wounds (Group I)*

CLSM imaging of normal skin showed the characteristic features of SC appearing as a bright somewhat cohesive layer, arranged in typical fields, folds, and furrows. At the level of the dermoepidermal junction dermal papillae with dark appearance surrounded by a rim of somewhat bright basal cells were visualized. Within dermal papillae capillaries seen as bright canalicular structures are observed (Fig. 1, normal skin). Real-time imaging of normal skin showed regular blood flow within the blood vessels of the dermal papillae without significant leukocyte-endothelial interaction (Video 1, Quick time, 1.4 MB).

CLSM imaging of the test site 30 min after cryotherapy showed an increased distension of skin folds and furrows, while respecting the original architecture and tension lines. At the level of the spinous layer CLSM identified focal areas with thickened and blurred intercellular demarcations (Fig. 2) likely corresponding to early spongiosis. CLSM imaging at the level of the DEJ showed less well-defined dermal papillae and some blood vessels.

Table 2 CLSM evaluation parameters. Morphological aspects of CLSM analysis based on established histological features in comparison to normal skin. The abscence/presence of respective CLSM features was recorded during in vivo examination and by retrospective image analysis. Semiquantitative scoring was performed for chronic skin wounds, whereby a score of 0 = none, 1 = mild, 2 = moderate, and 3 = severe was assigned to individual patients.

CLSM parameter	Group I	Group II	Group III
Epidermis	Loss of SC integrity after blister removal Stage of re-epithelialization Restoration of SC integrity	Visualization of slough formation-Inflammatory infiltrate Impetiginization	Morphology/integrity of epidermal architecture
	Architectural changes in granular/spinous/basal layer Dermoepidermal junction	Stage of re-epithelialization Presence of keratinocytes Presence of corneocytes	Stage of re-epithelialization-Presence of keratinocytes
	Spongiosis, Exocytosis (presence/absence)	Morphology of adjacent epidermal keratinocytes	Spongiosis, exocytosis (semiquantitative scoring)
Dermis	Superficial dermal capillariesNumber/morphology (dilatation/elongation)	Superficial dermal capillaries Number/morphology (dilatation/elongation)	Superficial dermal capillaries Number/morphology (dilatation/elongation)
	Inflammatory infiltrate	Inflammatory infiltrate	Inflammatory infiltrate (semiquantitative scoring)
	Reactive changes in subjacent dermal tissue inflammatory infiltrate Morphology of collagen bundles	Morphology of collagen bundles Scar formation/presence of fibrosis	Morphology of collagen bundles

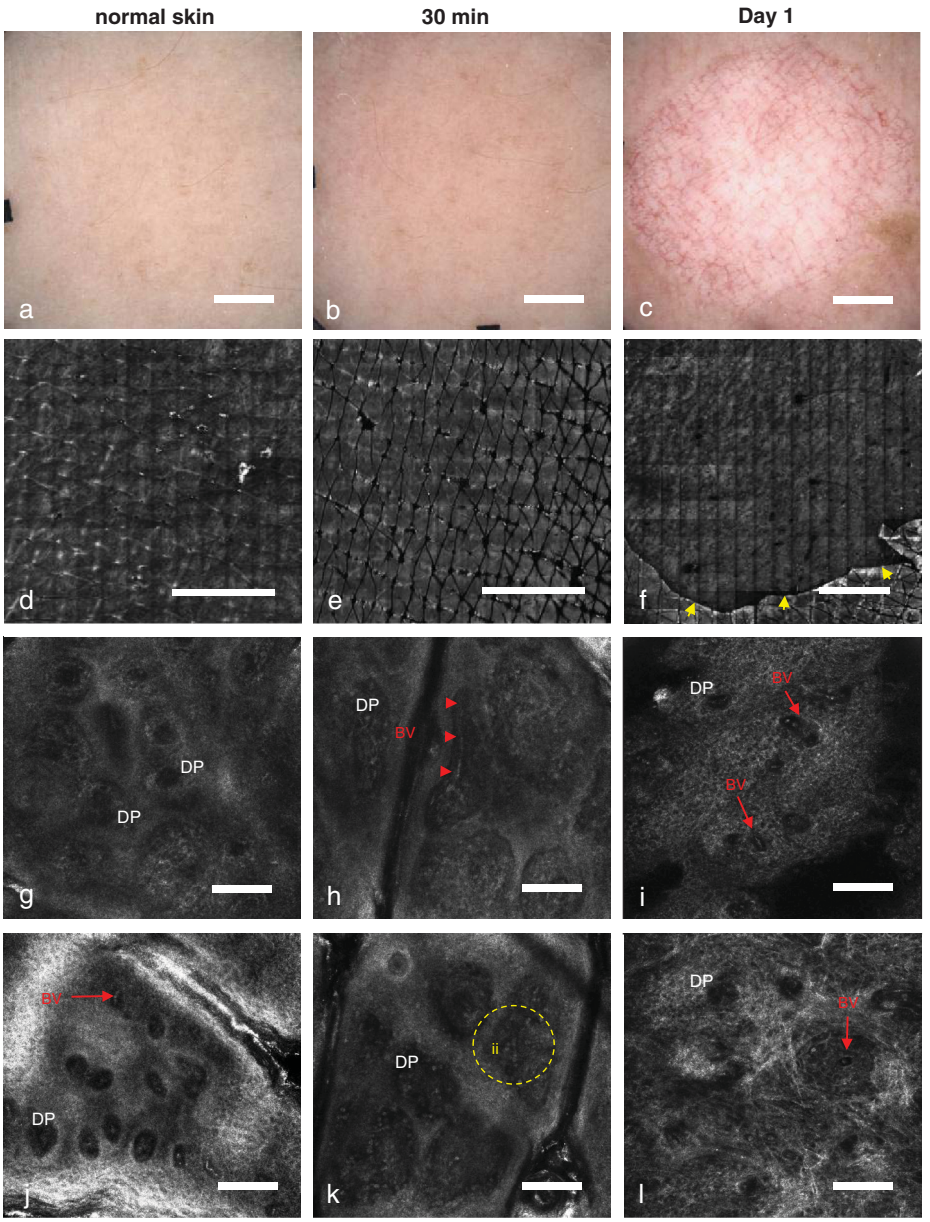

Fig. 1 CLSM evaluation of superficial epidermal wounds up to day 1 (inflammatory phase of wound healing). Normal skin: (a) Macroscopic image showing test site with normal skin prior to cryotherapy. (d) CLSM images (Vivablock™) obtained at the level of the stratum corneum (SC) with characteristic skin folds and furrows seen as dark horizontal lines intersecting fields of aggregated corneocytes. (g) CLSM imaging at the level of the dermoepidermal junction (DEJ) shows dermal papillae (DP) as dark round areas surrounded by somewhat bright rims of basal cells ($z = 41$ μm). Within the underlying papillary dermis, dermal papillae are seen as dark round areas (DP). The image is obtained from the superficial dermis as indicated by the presence of basal keratinocyte patches. (j) Occasionally, some blood vessels (BV, red arrow) are pictured ($z = 55$ μm). Thirty min after cryotherapy: (b) Macroscopic image showing faint erythema shortly after cryotherapy. (e) CLSM overview (Vivablock™) shows distension of the folds and furrows. (h) At the level of the DEJ, CLSM imaging shows less well-defined dermal papillae and some blood vessels are visible (BV, red arrowheads) ($z = 45$ μm). (k) At the level of the superficial dermis inflammatory cells are distributed mainly within the dermal papillae (ii, yellow dashed circle) ($z = 60$ μm). Day 1 after cryosurgery and removal of the epidermal blister roof. (c) Macroscopic image showing round circumferential defect of epidermis. (f) CLSM imaging at the level of the stratum corneum (SC) shows a corresponding epidermal defect with sharp demarcation to surrounding skin (yellow arrowheads). (i) At the level of the DEJ, regular junctional architecture seems disrupted and blood flow may be visualized with dermal capillaries ($z = 0$ μm). (l) At the level of the superficial dermis, fibrous structures appear with increased brightness compared to normal skin ($z = 39$ μm). [Scale bars: (a) to (c): 2 mm; (d) to (f): 200 μm; and (g) to (l): 100 μm].

Real-time imaging showed increased blood flow in somewhat dilated vessels and presence of lymphocytes rolling along the blood vessel wall 30 min after cryo-induced damage (Video 2, Quick time 3.7 MB). The distinction of lymphocytes is based upon their larger diameter compared to that of erythrocytes in the surrounding blood flow (Fig. 1, 30 min) (Video 2, Quick time 3.7 MB). At the level of the superficial/papillary dermis mainly perivascular inflammatory infiltrate is observed.

Following blister removal on day 1, the superficial epidermal defect becomes visible on CLSM evaluation, by showing a central, well circumscribed dark area surrounded by the remaining SC with bright appearance. CLSM imaging at the level of the

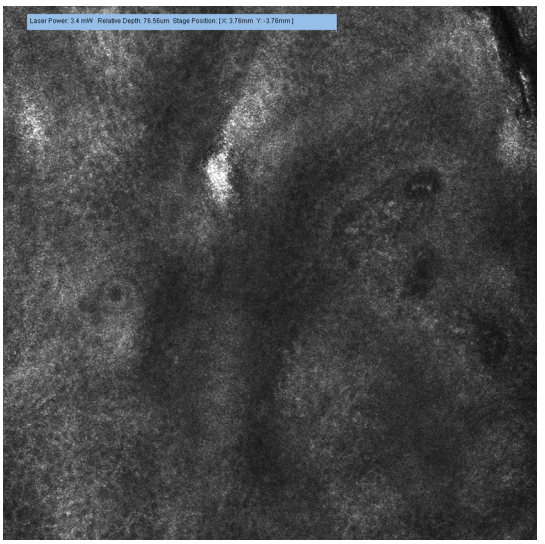

Video 1 Real-time images of normal skin showing the blood flow within the blood vessels of the papillae. The video sequence reveals no obvious signs of leukocyte-endothelial interaction such as intravascular rolling pattern of lymphocytes along the blood vessel wall. The blood vessels within the dark papillae seem regularly sized. (Quick time, 1.4 MB) [URL: http://dx.doi.org/10.1117/1.JBO.17.7.076016.1].

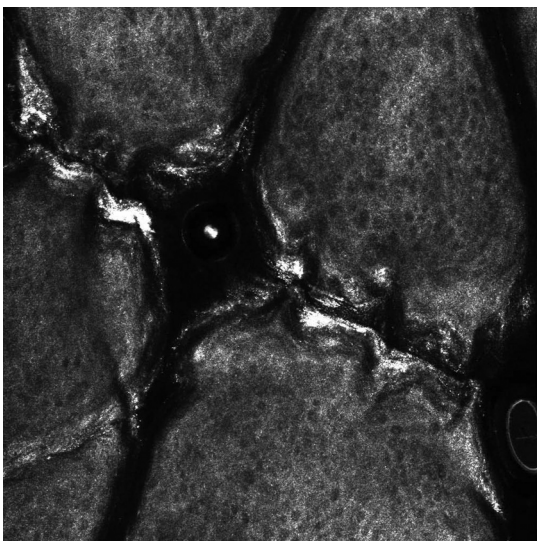

Fig. 2 Thirty minutes after the cryo-induced damage, focal areas with findings previously ascribed to spongiosis were observed, including thickened and blurred intercellular demarcations. Former CLSM studies related these characteristics to focal minimal to mild spongiosis.[18,20,21]

dermis showed ill-defined dermal papillae compared to normal skin, with noted increase of blood flow and elongation of superficial capillaries. The fibrous structures within the dermis showed increased brightness on CLSM evaluation, resulting in a more distinct appearance compared to normal skin (Fig. 1, day 1).

CLSM imaging on day 7 showed bright digitate protrusions from the wound margins corresponding to thin sheets of keratinocytes migrating towards the wound center. On individual images, these sheets correspond to loosely aggregated, somewhat elongated keratinocytes or fields of bright, polygonal corneocytes in CLSM evaluation (Fig. 3, day 7).

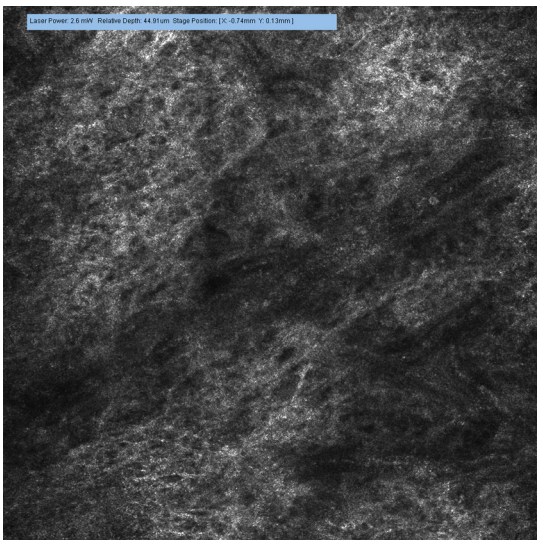

Video 2 Real-time images show the blood flow within the blood vessels of the dermal papillae 30 min after cryo-induced damage. The increased Intravascular rolling pattern of lymphocytes along the blood vessel wall of the dilated vessels are typical signs of inflammatory skin conditions. (Quick time, 3.7 MB) [URL: http://dx.doi.org/10.1117/1.JBO.17.7.076016.2].

CLSM imaging on day 14 showed continued wound closure, whereby only a small, residual epidermal defect may be visualized. At the level of the dermoepidermal junction, the restoration of a regular honeycomb pattern may be observed. In addition, sparse inflammatory cells and occasional presence of dendritic shaped bright cells were visualized. While the latter most likely correspond to epidermal dendritic cells, no further distinction may be made by CLSM. Within dermal papillae, superficial dermal capillaries were visualized in regular density and distribution. Dermal fibrous structures showed no apparent structural alteration, resembling the delicate network seen in normal skin (Fig. 3, day 14).

CLSM imaging at week 4 revealed complete re-epithelialization with regular epidermal and dermal architecture, and no residual inflammation (data not shown).

3.2 *CLSM Findings of Superficial Dermal Wounds (Group II)*

Clinical evaluation of split skin donor sites at day 5 revealed serohemorrhagic crusting of variable thickness and the formation of a preliminary wound matrix within the wound bed. CLSM imaging at the level of the wound surface revealed crusting/slough formation seen as amorphous bright area [Fig. 4(a) to 4(c)]. One patient showed the presence of block-like formations and areas of clefting, which appear to evolve under dry wound conditions [Fig. 4(b)]. In addition, numerous bright, round to oval structures of approximately 6 to 10 μm were visualized within the wound surface likely corresponding to inflammatory cells and cell remnants. While inflammatory cells have been described as bright, round to oval cells of approximately 8 to 10 μm, macrophages have previously been described as bright, roundish-plump cells of 12 to 15 microns in diameter.[22,23] Moreover, oblong or segmented bright cells, with 9 to 15 microns in diameter are seen on CLSM that might correspond to Polymorphonuclear cells [Fig. 4(c)].

CLSM evaluation within the wound matrix showed inflammatory cells in variable density in the absence of a regular

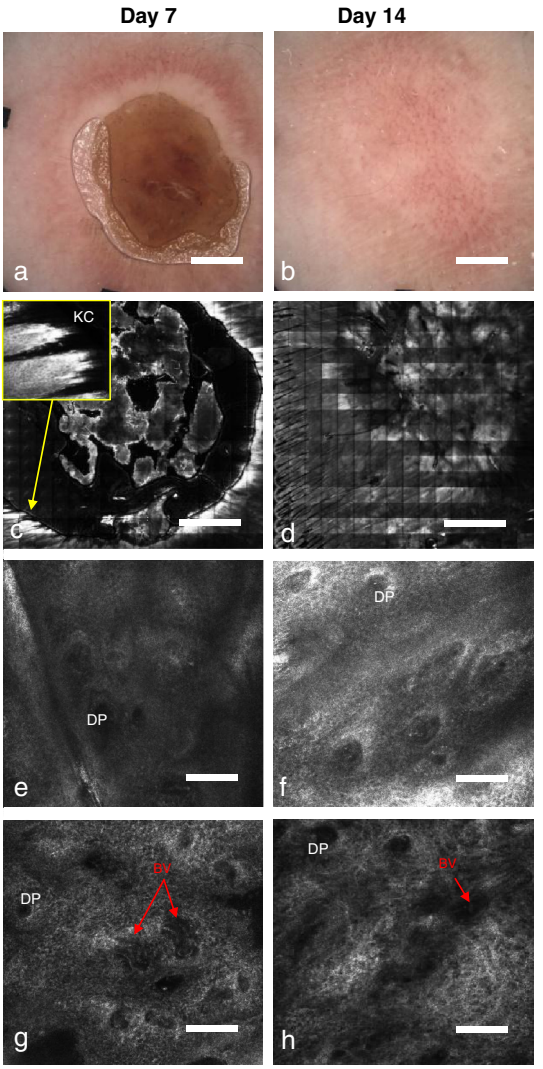

Fig. 3 CLSM evaluation of superficial epidermal wounds up to day 1 (tissue formation and remodelling phases). Day 7 after cryosurgery: (a) Macroscopic inspection shows marked scab formation. (c) CLSM imaging at the level of the SC shows consecutive wound closure and contractions of wound margins as well as crust formation. (c, detail upper left) Finger-like protrusions of keratinocytes (KC) migrate towards the center of the wound. (e) At the level of the DEJ dermal papillae (DP) show more regular appearance ($z = 49$ μm), whereas (g) elongated and tortuous blood vessels (BV, red arrows) are seen in the superficial dermis ($z = 80$ μm). Day 14 after cryosurgery: (b) Macroscopic inspection shows subtotal wound closure with faint residual erythema and postinflammatory hyperpigmentation. (d) CLSM imaging at the level of the SC demonstrates that the normal epidermal architecture of folds and furrows is not yet completely restored. (f) CLSM imaging at the level of the DEJ shows progressive normalization of junctional architecture with honeycombed pattern of surrounding basal keratinocytes and dermal papillae (DP) ($z = 54$ μm). (h) Within the dermis a delicate network of dermal fibrous structures of moderate brightness is seen, resembling that of normal skin; superficial dermal capillaries were visualized within some dermal papillae (BV, red arrow) ($z = 65$ μm). [Scale bars: (a) to (b): 2 mm; (c) (d): 200 μm; and (e) (h): 100 μm].

epidermis [Fig. 4(d) to 4(e)]. The detailed visualization of superficial dermal vasculature within the wound bed was only possible in cases with mild inflammation, minimal crusting, or in close vicinity to the wound margin [Fig. 4(f)]. Vasculature seemed elongated and widened compared to normal skin, appearing as bright, canalicular structures due to their content of erythrocytes and visible blood flow upon in vivo CLSM evaluation. In addition, inflammatory cells may be visualized in perivascular and interstitial distribution [Fig. 4(f)].

CLSM imaging at skin sites adjacent to the dermal wound showed spongiosis [Fig. 4(g) to 4(h)] and partial alteration of the adjacent epidermal architecture with elongation of granular keratinocytes due to incipient wound contraction [Fig. 4(h)]. The presence of aggregates of polygonal corneocytes corresponds to initial re-epithelialization protruding towards to wound center [Fig. 4(i)].

3.3 *CLSM Findings of Deep/Chronic Skin Wounds (Group III)*

The evaluation of chronic skin wounds included different subsets of patients; two ($n = 2$) patients with chronic skin ulcers with a history of poor response to topical therapy; two ($n = 2$) patients with chronic skin ulcers and a history of good response to therapy, rendering only residual superficial erosions for CLSM evaluation; lastly, the evaluation included one ($n = 1$) patient with a chronic skin ulcer following re-epithelialization under topical wound management.

In the subset studied during this evaluation, those patients with poor response to therapy showed a reduced or absent inflammatory infiltrate upon CLSM evaluation of wound margins within the epidermis and superficial dermis, while exhibiting marked spongiosis with granular and spinous layers (Fig. 5, Pat. 1). Those patients with moderate response to therapy featured spongiosis at the level of the granular and spinous layers, and presence of inflammatory cells in moderate density interspersed within keratinocytes and superficial dermis (Fig. 5, Pat. 2). One patient with early re-epithelialization showed marked inflammation with the presence of numerous round to oval bright cells interspersed between epidermal keratinocytes and superficial dermal collagen deposits (Fig. 5, Pat. 3). Spongiosis at the level of the spinous and granular layer was invariably present in all examined skin sites [Fig. 5(d) to 5(f)] while the level of extent varied between the studied subsets of patients.

CLSM images obtained at the level mid superficial dermal layer of all three patients show aggregates of fibrous structures seen as bright strands of variable thickness, arranged in a reticulated pattern and somewhat haphazard orientation. Patients with moderate and good wound healing show occasional round to oval bright inflammatory cells. The absence of well-defined dermal papillae indicates a loss of regular epidermal architecture and skin atrophy. Within the dermis increased vascularization may be seen by presence of elongated and/or dilated canalicular dermal blood vessels (Fig. 5).

4 Discussion

Cutaneous wound healing is a dynamic, well-orchestrated process involving soluble mediators, blood cells, extracellular matrix, and parenchymal cells. The process can be divided in three overlapping phases—inflammation, tissue formation, and tissue remodeling—and has been well described by histological analyses.[19]

During the *inflammatory phase* a provisional matrix is formed and infiltrating neutrophils clean the tissue of foreign particles and bacteria. Blood vessels in the wound bed are dilating. The phase of *tissue formation* is characterized by the formation of granulation tissue within the wound bed, consisting of migrating fibroblasts and angiogenesis[19] followed by the phase

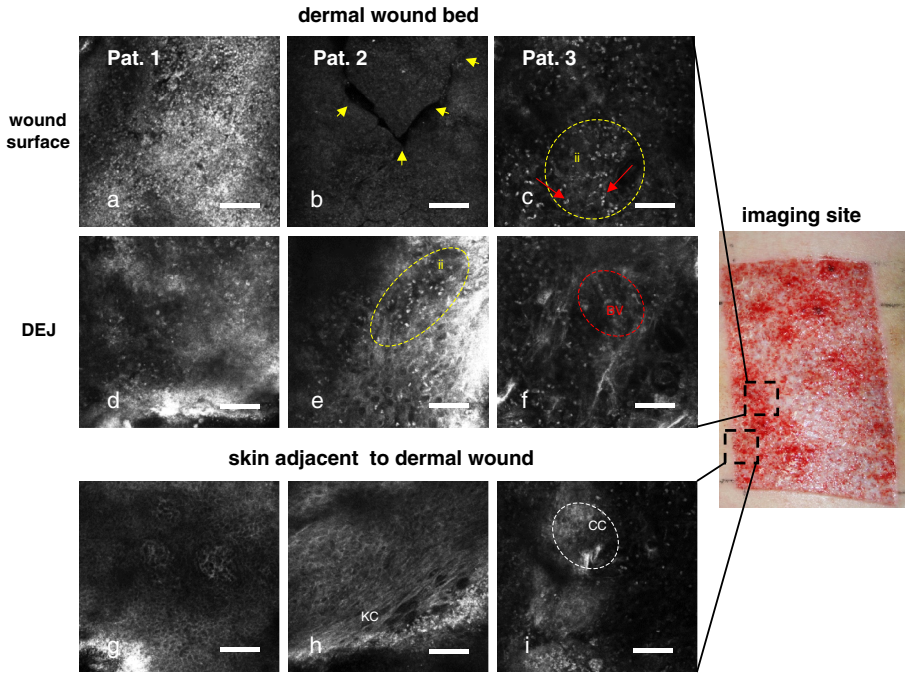

Fig. 4 CLSM evaluation of superficial dermal wounds of 3 different patients 5 days after wounding. Representative clinical photograph obtained from split skin donor sites at day 5 showing serohemorrhagic crusting and formation of a preliminary wound matrix. Imaging sites within dermal wound bed (a) to (f) and adjacent skin (g) to (i) are schematically indicated by dashed square. (a) to (c) CLSM images obtained from the wound bed surface illustrating superficial slough formation/crusting seen as unstructured area of low refractillity (b) sometimes forming cleft-like spaces of dark appearance (yellow arrowheads). Variable presence of inflammatory infiltrate seen as scattered bright, round to oval cells (a, c) (dashed yellow circle, ii). (c) The inflammatory infiltrate partly resembles PMN due to the segmented nuclei (red arrows). CLSM imaging at the level of the dermoepidermal junction (DEJ) revealed inflammatory infiltrate as bright round to oval cells within the preliminary wound matrix (images d, e) (dashed yellow circle, ii). (f) CLSM imaging at the level of the superficial dermis showed some dilated capillaries (BV), seen as bright, elongated canalicular structure (BV, red dashed circle). Concomitant inflammatory infiltrate may be visualized as bright round to oval cells in perivascular and interstitial distribution. Representative CLSM images obtained from adjacent untreated skin areas showing (g) aspects of normal glarebral skin and (h) somewhat elongated keratinocytes (KC) with some mild degree of spongiosis seens as increased intercellular brightness. CLSM image (i) shows aggregates of large, polygonal corneocytes (CC, dashed white circle) and residual inflammatory cells consistent with incipient re-epithelialization. (Scale bars: 100 μm)

of tissue remodeling. *Tissue remodeling* is characterized by the controlled restitution of blood vessels in the granulation tissue as a result of apoptosis and increasing collagen synthesis and deposition within the wound matrix.

Using the model of cryosurgery induced *epidermal wounds*, the process of epidermal tissue repair was studied by serial CLSM evaluations of the wound bed and wound margin, beginning at superficial layers and reaching into the upper dermis. CLSM was able to visualize the consecutive events of wound formation and wound healing, from loss of SC integrity until complete re-epithelialization. At the early phase of skin response inflammatory cells were seen within the epidermis, while the presence of a honeycombed pattern corresponded to the restoration of normal epidermal architecture at day 14. Thirty minutes after the cryo-induced damage, focal areas with findings previously ascribed to spongiosis were observed, including thickened and blurred intercellular demarcations. Previous CLSM studies related these characteristics to focal minimal to mild spongiosis.[18,20,21]

Interestingly, although cryo-induced skin wounds are limited to the epidermis upon clinical inspection, CLSM was able to visualize transient alterations of dermal papillae and superficial dermal vasculature. Upon sequential CLSM imaging leukocyte-endothelial interactions were observed as rolling and tethering of lymphocytes (Video 2, Quick time 3.7 MB). The presence of these intravascular lymphocytes and the dermal inflammatory infiltrate [Fig. 1(k)] may represent reactive changes as part of the local inflammatory response as it has been described in inflammatory skin conditions.[24]

The resolution of CLSM images allowed a morphological description of the inflammatory phase (day 1) dominated by exocytosis. The tissue formation phase was characterized by CLSM showing reactive keratinocyte proliferation and their progressive migration into the wound bed from the surrounding wound margin. Thereby, CLSM was able to monitor the process of re-epithelialization over time. During the phase of tissue remodeling, CLSM allowed for the visualization of the progressive normalization of the dermoepidermal architecture with formation of a regular honeycombed pattern and the restoration of all epidermal layers between days 7 and 14. Occasional dendritic cells found 14 days after injury might correspond to epidermal dendritic cells repopulating the regenerating epidermis.[25]

Therefore, CLSM enables the investigator to observe the onset of inflammation, the dynamics of wound closure, and the time point of completed tissue repair. Our findings are confirmatory of preliminary investigations using CLSM in the evaluation of epidermal wounds and previous studies using fluorescence CLSM for the evaluation of wound repair in suction blisters. In these studies, morphologic features of the individual phases of tissue repair were visualized, thereby defining the respective stages of wound healing over time.[26,27]

Next, we set out to study the applicability of CLSM for the evaluation of wound healing in *superficial dermal wounds*. For that purpose we have chosen the split skin grafts donor site

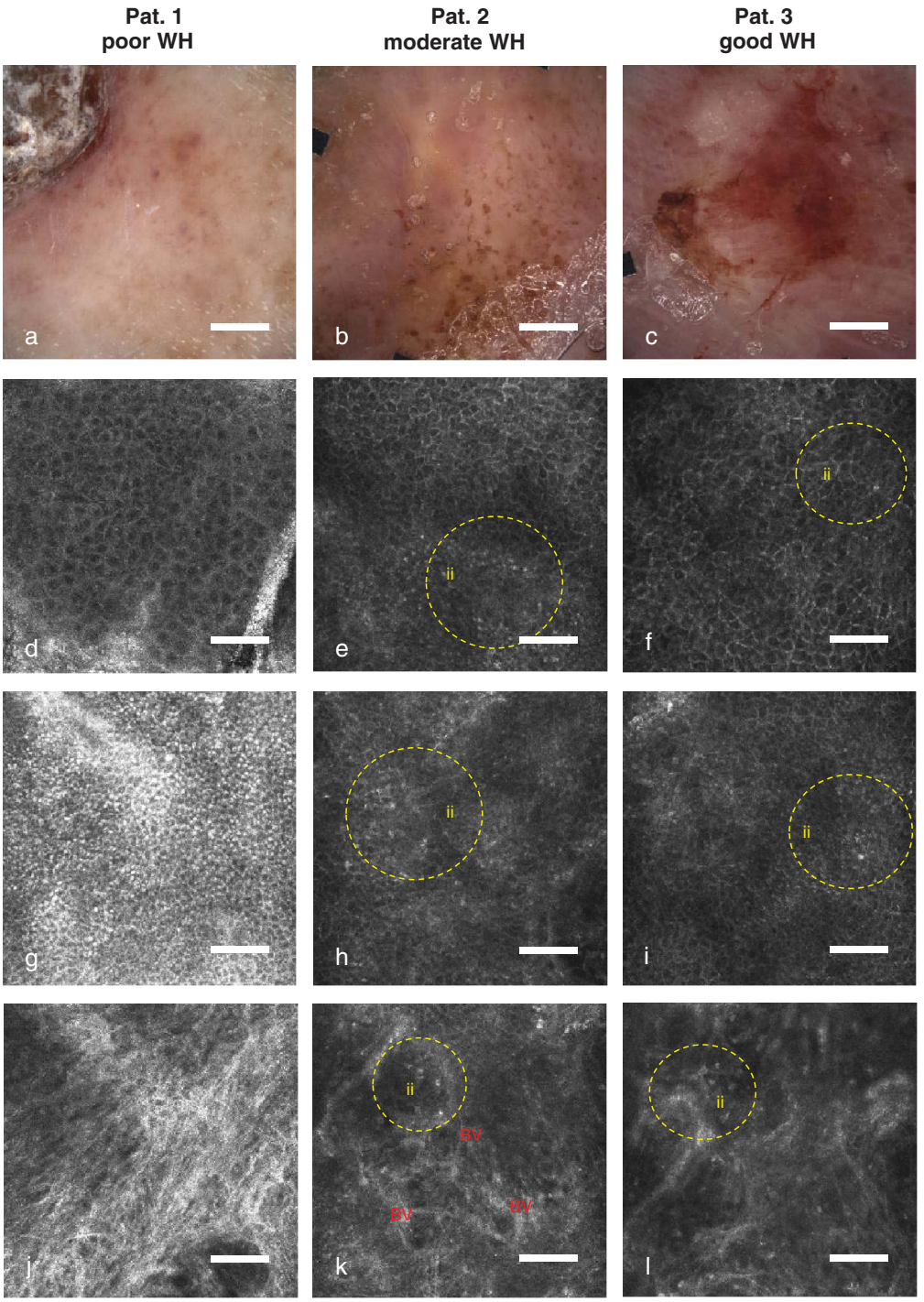

Fig. 5 CLSM evaluation of skin adjacent to chronic deep dermal wounds. CLSM images were obtained from respective wound margins in three patients with different healing tendencies. Patient 1 presented with a chronic ulcer and a history of poor response to therapy. (a) Macroscopic inspection revealed indurated skin with some areas of hyperpigmentation. (d) CLSM images obtained at the granular layer (SG) illustrate moderate spongiosis and absence of inflammatory cells. (g) At the level of the suprabasal layer increased brightness of basal cells, corresponding to hyperpigmentation, is observed. (j) CLSM images obtained at the level mid superficial dermis shows aggregates of bright, reticulated fibrous structures in somewhat haphazard orientation and distribution and absence of inflammatory cells.Patient 2 showed moderate signs of wound healing. (b) Macroscopically erythema and hyperpigmentation are present. Within the SG mild to moderate spongiosis pattern is observed. (e) Presence of inflammatory infiltrate (ii) seen as round-to-oval bright cells interspersed within granular keratinocytes (dashed yellow circle). (h) CLSM image obtained from within the spinous layer illustrating spongiosis with pronounced inflammatory infiltrate (ii, yellow arrowheads) interspersed within spinous/basal keratinocytes. (k) Images obtained at the level of the mid superficial dermis showing fibrous bundles of moderate brightness and occasional round to oval bright cells inflammatory infiltrate (ii, dashed yellow circle). Increased vascularization seen by presence of numerous dermal blood vessels (BV). Patient 3 showed good signs of wound healing. (c) Macroscopic inspection showed noted erythema and hyperpigmentation. (f) CLSM images obtained from the SG illustrate spongiosis and presence of inflammatory cells (ii, dashed yellow circle). (i) CLSM images obtained from the spinous layer (SS) illustrating moderate-marked spongiosis and inflammatory infiltrate (ii, dashed yellow circle). (l) CLSM images obtained at the level of the dermis illustrate elongation and dilatation of dermal blood vessels. The loss of dermal papillae indicates disruption of regular architecture and skin atrophy (l). Pronounced inflammatory infiltrate (ii, dashed yellow circle) is found in the dermis combined with fibrous structures in haphazard distribution. [Scale bars: (a) to (c): 2 mm; and (d) to (l): 100 μm.]

model as representative to investigate the classical evolution of wound healing in a clinical setting. The harvesting of the skin with a dermatome allows the creation of wounds, standardized in surface area and depth. Following the mechanical removal of the epidermis, the wound surface consists of slough and subjacent dermis. CLSM enabled the visualization of slough as an amorphous bright structure of moderate refractility containing numerous round to oval bright cells that, due to their segmented appearance, might correspond to polymorphonuclear cells and cell remnants.

Although neutrophils might delay the closure of artificial, microbiologically sterile wounds[28,29] their inevitable role in cutaneous wound healing has been well described.[29]

While CLSM has already been established for investigations of the biofilm *in vitro*,[30–33] it remains to be elucidated whether *in vivo* CLSM could be used for biofilm research of wounds and other surfaces of the body. In our studies, CLSM was suitable for the visualization of the inflammatory cells within the dermis and for the evaluation of incipient re-epithelialization along the wound margins. At day 5, aspects of neovascularization as well as re-epithelialization were found at the wound edge.

Based on these findings the inflammatory phase and the tissue formation phase seem to overlap in dermal wounds at day 5. This is supportive of previous findings from routine histology at this timepoint.[19] For the purpose of this study, we did not evaluate the phase of tissue remodeling.Therefore, no conclusions may be drawn as to the influence of local inflammation on the structural and cosmetic outcome of individual test sites.

Another goal of this investigation was to test the feasibility of CLSM for the evaluation of deep dermal skin wounds, including patients with chronic venous leg ulcers. Not unexpectedly, CLSM was unable to evaluate the area of the wound bed due to significant slough formation, limiting the analysis to the respective wound margins. While the wound edge is the starting point for the migration of keratinocytes into the wound bed, it is also exposed to the aggressive and proteolytic environment of the adjacent wound bed.[34,35] The latter may significantly reduce the regenerative potential of the wound margin, ultimately leading to a lack of re-epithelialization. Therefore, the evaluation of the wound edge and the surrounding skin gives valuable information to the clinician and allows for individual adaptation of the wound management protocol.

Considering the heterogeneity of evaluated patients, it was not surprising to find a broad variety of CLSM findings corresponding to the inflammation, re-epithelialization, and the remodeling at the wound edge.

In those wounds with good healing, polygonal granular keratinocytes and thin, more or less cohesive sheets of corneocytes were found which are consistent with incipient re-epithelialization. The wound margins also showed signs of tissue remodelling, such as increased vascularization and aspects of fibrosis. In addition, CLSM was able to show the loss of the dermal papillae, indicating the disruption of the regular architecture. This feature of tissue remodelling is also found in stasis dermatitis, as it occurs in patients suffering from chronic venous insufficiency.

From the small subset of patients evaluated, however, we did see a trend towards increased inflammation in wounds with good healing tendency, as opposed to nonhealing skin ulcers, showing almost no inflammatory cells and only mild spongiosis. Although there is not much evidence, it may be speculated, whether a certain amount and composition of inflammatory infiltrate might be necessary for the wound healing process as the inflammation phase is the earliest phase in tissue repair.

Overall, the findings of this investigation indicate that CLSM may serve as an adjunct noninvasive diagnostic tool for the evaluation of cutaneous wound healing. With a resolution that is comparable to routine histology, cellular, and morphological details of superficial and deep, acute and chronic skin wounds may be visualized, whereby aspects of inflammation, vascularization, and re-epithelialization may be documented on a cellular level. CLSM allows a semiquantitative analysis of the extent of edema and inflammatory infiltrate, thereby giving important information about the individual healing phase and stage of epithelialization. However, in contrast to immunohistochemical analysis in routine histology, CLSM cannot differentiate between the inflammatory cells *in vivo*. Moreover, the image analysis is inherently subjective. This limitation is addressed by a number of research groups investigating the use of computer-assisted analysis of CLSM images.[36–38]

With an imaging area of 8×8 mm, CLSM is particularly suitable for the evaluation of small experimental wounds since the entire wound geography including the fine layers of emerging epithelialization can be evaluated over time. Based on the experience of this study, CLSM imaging may include an assessment of the wound closure rate. Moreover, functional parameters such as the measurement of the blood flow and the adherence of inflammatory cells to the blood vessel walls might be valuable in future studies.

Overall, superficial epidermal wounds are most suited for noninvasive evaluation. The CLSM evaluations of the wound bed of superficial and deep dermal wounds, however, were complicated by variable crust/slough formation and the presence of mild-to-moderate exudate following surgery. Thus, the placement and immobilization of the CLSM objective posed a significant challenge, ultimately interfering with an evaluation of underlying dermal structures.

In summary, CLSM may contribute to an understanding of the consecutive events of wound healing and assist in the morphological analysis of skin wounds on a microscopic level. Considering respective limitations, different techniques may be used complementary for comprehensive wound analysis and may ultimately play a role in the prognostic assessment and therapeutic management of acute and chronic skin wounds. In that regard, the role of CLSM with respect to wound healing may include pharmacological testing of topical drugs and wound dressings, including the observation of product related side-effects *in vivo*, thereby avoiding risks potentially associated with histomorphological evaluations.

References

1. R. G. Sibbald et al., "Preparing the wound bed—debridement, bacterial balance, and moisture balance," *Ostomy Wound Manage* **46**(11), 14–22, 24–18, 30–15 (2000).
2. S. Enoch, J. E. Grey, and K. G. Harding, "ABC of wound healing. Non-surgical and drug treatments," *BMJ* **332**(7546), 900–903 (2006).
3. C. T. Hess and R. S. Kirsner, "Orchestrating wound healing: assessing and preparing the wound bed," *Adv. Skin Wound Care* **16**(5), 246–257 (2003).
4. J. Panuncialman et al., "Wound edge biopsy sites in chronic wounds heal rapidly and do not result in delayed overall healing of the wounds," *Wound Repair Regen.* **18**(1), 21–25 (2010).
5. J. M. Davidson, "Animal models for wound repair," *Arch. Dermatol. Res.* **290**(14), S1–S11 (1998).

6. A. Scheid et al., "Genetically modified mouse models in studies on cutaneous wound healing," *Exp. Physiol.* **85**(6), 687–704 (2000).
7. R. C. Fang and T. A. Mustoe, "Animal models of wound healing: utility in transgenic mice," *J. Biomater. Sci. Polym. Ed.* **19**(8), 989–1005 (2008).
8. Y. K. Hong et al., "VEGF-A promotes tissue repair-associated lymphatic vessel formation via VEGFR-2 and the alpha1beta1 and alpha2beta1 integrins," *FASEB J.* **18**(10), 1111–1113 (2004).
9. R. Mani, "Science of measurements in wound healing," *Wound Repair Regen.* **7**(5), 330–334 (1999).
10. S. Astner et al., "Non-invasive evaluation of the kinetics of allergic and irritant contact dermatitis," *J. Invest. Dermatol.* **124**(2), 351–359 (2005).
11. M. A. Altintas et al., "Differentiation of superficial-partial vs. deep-partial thickness burn injuries in vivo by confocal-laser-scanning microscopy," *Burns* **35**(1), 80–86 (2009).
12. A. A. Altintas et al., "To heal or not to heal: predictive value of in vivo reflectance-mode confocal microscopy in assessing healing course of human burn wounds," *J. Burn Care Res.* **30**(6), 1007–1012 (2009).
13. D. Ratner, "Skin grafting," *Semin. Cutan. Med. Surg.* **22**(4), 295–305 (2003).
14. R. G. Sibbald et al., "Special considerations in wound bed preparation 2011: an update(c)," *Adv. Skin Wound Care* **24**(9), 415–436; quiz 437–418 (2011).
15. M. Ulrich et al., "Reflectance confocal microscopy for noninvasive monitoring of therapy and detection of subclinical actinic keratoses," *Dermatology* **220**(1), 15–24 (2010).
16. M. Rajadhyaksha, R. R. Anderson, and R. H. Webb, "Video-rate confocal scanning laser microscope for imaging human tissues in vivo," *Appl. Opt.* **38**(10), 2105–2115 (1999).
17. M. Rajadhyaksha et al., "In vivo confocal scanning laser microscopy of human skin II: advances in instrumentation and comparison with histology," *J. Invest. Dermatol.* **113**(3), 293–303 (1999).
18. K. Swindells et al., "Reflectance confocal microscopy may differentiate acute allergic and irritant contact dermatitis in vivo," *J. Am. Acad. Dermatol.* **50**(2), 220–228 (2004).
19. A. J. Singer and R. A. Clark, "Cutaneous wound healing," *N. Engl. J. Med.* **341**(10), 738–746 (1999).
20. S. Gonzalez et al., "Characterization of psoriasis in vivo by reflectance confocal microscopy," *J. Med.* **30**(5–6), 337–356 (1999).
21. S. Gonzalez et al., "Allergic contact dermatitis: correlation of in vivo confocal imaging to routine histology," *J. Am. Acad. Dermatol.* **40**(5, Pt. 1), 708–713 (1999).
22. P. Guitera et al., "Morphologic features of melanophages under in vivo reflectance confocal microscopy," *Arch. Dermatol.* **146**(5), 492–498 (2010).
23. K. J. Busam et al., "Morphologic features of melanocytes, pigmented keratinocytes, and melanophages by in vivo confocal scanning laser microscopy," *Mod. Pathol.* **14**(9), 862–868 (2001).
24. S. Gonzalez et al., "Real-time evidence of in vivo leukocyte trafficking in human skin by reflectance confocal microscopy," *J. Invest. Dermatol.* **117**(2), 384–386 (2001).
25. M. Demarchez, D. Asselineau, and J. Czernielewski, "Migration of Langerhans cells into human epidermis of "reconstructed" skin, normal skin, or healing skin, after grafting onto the nude mouse," *J. Invest. Dermatol.* **100**(5), 648–652 (1993).
26. B. Lange-Asschenfeldt et al., "Effects of a topically applied wound ointment on epidermal wound healing studied by in vivo fluorescence laser scanning microscopy analysis," *J. Biomed. Opt.* **14**(5), 054001 (2009).
27. D. Terhorst et al., "Reflectance confocal microscopy for the evaluation of acute epidermal wound healing," *Wound Repair Regen.* **19**(6), 671–679 (2011).
28. J. V. Dovi, A. M. Szpaderska, and L. A. DiPietro, "Neutrophil function in the healing wound: adding insult to injury?," *Thromb Haemost.* **92**(2), 275–280 (2004).
29. C. Nathan, "Neutrophils and immunity: challenges and opportunities," *Nat. Rev. Immunol.* **6**(3), 173–182 (2006).
30. A. N. Gurjala et al., "Development of a novel, highly quantitative in vivo model for the study of biofilm-impaired cutaneous wound healing," *Wound Repair Regen.* **19**(3), 400–410 (2011).
31. B. Guggenheim et al., "Application of the Zurich biofilm model to problems of cariology," *Caries Res.* **38**(3), 212–222 (2004).
32. T. R. Neu et al., "Advanced imaging techniques for assessment of structure, composition and function in biofilm systems," *FEMS Microbiol. Ecol.* **72**(1), 1–21 (2010).
33. J. R. Lawrence et al., "Optical sectioning of microbial biofilms," *J. Bacteriol.* **173**(20), 6558–6567 (1991).
34. S. M. McCarty et al., "The role of endogenous and exogenous enzymes in chronic wounds: a focus on the implications of aberrant levels of both host and bacterial proteases in wound healing," *Wound Repair Regen.* **20**(2), 125–136 (2012).
35. M. De Mattei et al., "Time- and dose-dependent effects of chronic wound fluid on human adult dermal fibroblasts," *Dermatol. Surg.* **34**(3), 347–356 (2008).
36. A. Lorber et al., "Correlation of image analysis features and visual morphology in melanocytic skin tumours using in vivo confocal laser scanning microscopy," *Skin Res. Technol.* **15**(2), 237–241 (2009).
37. A. Gerger et al., "Diagnostic image analysis of malignant melanoma in in vivo confocal laser-scanning microscopy: a preliminary study," *Skin Res. Technol.* **14**(3), 359–363 (2008).
38. M. Wiltgen et al., "Automatic identification of diagnostic significant regions in confocal laser scanning microscopy of melanocytic skin tumors," *Methods Inf. Med.* **47**(1), 14–25 (2008).